Agostino Stilli, Luca Grattarola, Hauke Feldmann, Helge A. Wurdemann, and Kaspar Althoefer. "Variable Stiffness Link (VSL): Toward inherently safe robotic manipulators." In Robotics and Automation (ICRA), 2017 IEEE International Conference on, pp. 4971-4976. IEEE, 2017.(DOI: 10.1109/ICRA.2017.7989578)

Variable Stiffness Link (VSL): Toward Inherently Safe Robotic Manipulators

Agostino Stilli, Luca Grattarola, Hauke Feldmann,
Helge A. Wurdemann and Kaspar Althoefer, *Member, IEEE*

***Abstract* — Nowadays, the field of industrial robotics focuses particularly on collaborative robots that are able to work closely together with a human worker in an inherently safe way. To detect and prevent harmful collisions, a number of solutions both from the actuation and sensing sides have been suggested. However, due to the rigid body structures of the majority of systems, the risk of harmful collisions with human operators in a collaborative environment remains.**

In this paper, we propose a novel concept for a collaborative robot made of Variable Stiffness Links (VSLs). The idea is to use a combination of silicone based structures and fabric materials to create stiffness-controllable links that are pneumatically actuated. According to the application, it is possible to change the stiffness of the links by varying the value of pressure inside their structure. Moreover, the pressure readings from the pressure sensors inside the regulators can be utilised to detect collisions between the manipulator body and a human worker, for instance. A set of experiments are performed with the aim to assess the performance of the VSL when embedded in a robotic manipulator. The effects of different loads and pressures on the workspace of the manipulator are evaluated together with the efficiency of the collision detection control system and hardware.

I. Introduction

At the dawn of industrial robotics, due to safety requirements, humans and robots were not sharing the same workspace, having manipulators usually confined in cages and fences. However, in the past decades, extensive research has focused on the development of software and hardware offering solution for inherently safe close human-robot interactions [1], [2]. In these shared working environments, safety for the human worker is of paramount importance that should be considered in the design of collaborative robots. In particular, a wide range of applications that are at present executed manually could benefit from a new generation of collaborative robots that allow safe close collaboration between the robot and the worker [3], [4].

* The research has received funding from the European Commission's project Horizon 2020 Research and Innovation Programme, project FourByThree under grant agreement No 637095.

A. Stilli, L. Grattarola are with the Department of Informatics, King's College London, Strand, London WC2R 2LS, UK (e-mail:{agostino.stilli, luca.grattarola}@kcl.ac.uk).

H. Feldmann is with the Faculty of Technology, Hochschule Emden/Leer, Constantiapl. 4, 26723 Emden, Germany (e-mail: feldmann.hauke@gmail.com)

H.A. Wurdemann is with is with the Department of Mechanical Engineering, University College London, Gower St, London WC1E 6BT, UK (e-mail: h.wurdemann@ucl.ac.uk).

K. Althoefer is with the School of Electronic Engineering & Computer Science, Queen Mary University of London, Mile End Rd, London E1 4NS, UK (e-mail: k.althoefer@qmul.ac.uk).

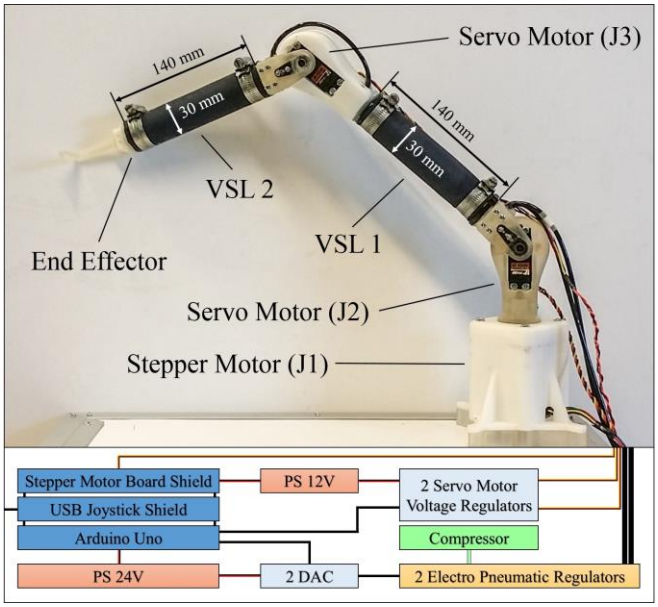

Figure 1 – Conceptual architecture of the anthropomorphic manipulator developed to assess the performance of the VSL.

Industrial robotic manipulators are typically high-payload machines, leading to a considerable robot body mass in comparison with the average body mass of a human being [5], [6]. Furthermore, they are usually capable of considerable accelerations and speeds (joints speed up to 160°/s with angular accelerations up to 100°/s^2 [5], [6]). In case of accidental collisions with a human worker, current industrial robots can exert potentially harmful or life-threatening forces to the human body [7], [8]. Hence, the field of industrial robotics is experiencing a paradigm shift from the traditional heavy-duty robot operating separated from the human worker in a fenced area, to robots that work closely with the human. The trend moves towards lightweight robots – examples include the Universal Robots UR5/UR10 [9], the lightweight robots from KUKA [5], FerRobotics [10], Franka [11], and the dual arm Baxter robot from Rethink Robotics [12]. These robotic manipulators claim to be safe due to integrated stiffness-controllable actuators that can adapt stiffness based on software tools that rely on sensory information.

In the attempt to make robots safer for interaction with humans, one of the first explored approaches was the development of variable stiffness actuators (VSA) [13], [14], given the rigid components of traditional manipulators. The electrical current and voltage response of electro-mechanical actuators to mechanical load variations allow to use these systems as intrinsic sensors within robotic manipulators

[15]; allowing faster and safer motion control with the aim of maximizing the motion speed while limiting risks of injury. A number of studies have confirmed that variable stiffness plays a key role to safe high performance. They address the safe human-robot interaction problem by extending the variable stiffness behaviour to the robot's joints (VSJ) [16]–[18]. The main aim of the control systems developed based on this new joint class is to minimize the probability of injuries due to unexpected collision with humans by taking advantage of the natural flexibility of the joints, absorbing potential impacts on the rigid components of the robot.

Sensing-based safety approaches have also been investigated, e.g. the use of distributed sensors on the external surface of the robot body [19]. These range from robot skins, providing contact recognition capabilities e.g. using pneumatic network [20] or capacitive sensors [21], to vision-based systems developed to avoid/detect collisions [22]. However, despite being very accurate in detecting the location and intensity of collision, these solutions share the need for additional hardware, a fact which can increase the price of the manipulator or limit its motion.

Although a lot has been done to improve sensors and actuators' performance for faster, safer and more accurate collision detection, limited efforts have been put into improving the intrinsic level of safety of the manipulator's links. Passive solutions like soft coatings and skins have been developed to provide a softer contact surface in case of accidental collisions by several robotics companies. However, the materials used to construct links of these "lightweight" robots have rigid properties. Metallic alloys and rigid polymers are used to build the core structure. Any collisions between a manipulator made of these materials and a human worker could result in serious traumas [23].

In this paper, we propose a novel design to effectively change and actively control the level of stiffness of robotic manipulators using the Variable Stiffness Link (VSL). Our system based on the VSL is able to actively tune the link's stiffness and to act as a distributed sensor for collision detection. In the proof of concept presented in this work, traditional rotational joints have been combined with pneumatically actuated VSLs composed of silicone, plastic meshes and fabric. In one of the first attempts to combine soft and traditional robotic elements bridging the current gap between the two in industrial robots, we propose a novel hybrid manipulator with the objective of increasing safety in human-robot interaction while being able to ensure high stiffness when required. As a result, not only can this manipulator be tuned from a completely soft to a rigid state according to the requirements of the task at hand, but collisions can also be detected without the need for additional sensors. Section II presents the VSL and the overall system design, working principle and fabrication process. A number of experiments have been conducted to evaluate both the workspace of the two links system and the collision detection algorithm developed which are presented along with the relative results in Section III. Section IV summarizes the achievements of this paper and presents future works.

II. Design and Fabrication Methodology

The presented robot comprises three off-the-self rotary actuators and two VSLs. The VSLs have been designed to:

- allow continuous stiffness tuning.
- withstand considerable forces (up to 2 N of tip load) without significantly deforming or collapsing.
- act as a distributed sensor and be intrinsically able to detect collisions.
- be scalable according to the size of the manipulator and to the required application's specification

The working principle and design of the VSL is inspired by our work on the inflatable manipulator firstly presented in [24], [25] and builds on the work proposed in [26]. The design has been optimised so that the available space inside the links is maximised providing internal channels for electrical cables, tendons or pressure lines to control motors and end effector tools (e.g., a gripper),

In this section the working principle of the VSL will be described in detail as well as the fabrication process and the assembly of the robotic manipulator.

A. VSL Working Principle and Design

The working principle of the VSL is summarized in Figure 2.a. The VSL is effectively a cylindrical air-tight chamber made of silicone encapsulated inside a fabric layer. In addition, a plastic mesh is embedded in between two layers of silicone as shown in Figure 2(a) and (b). Applying positive pressure to this chamber (as indicated by the double white arrow) results in the VSL to vary its stiffness as illustrated by the light blue arrows showing the direction of the pressure force of the air on the lateral walls of the cylinder. Typically, silicone-based soft robotic systems are subject to a phenomena called "ballooning". In some cases, this effect is not desirable, challenging to be modelled and might interfere with sensor performances. Here, the outer fabric layer reinforces the axial expansion of the VSL and prevents silicone deformation. Hence, higher pressures lead to greater forces, and thus greater stiffness of the link. At low pressure, the plastic mesh adds structural strength and prevents the link from collapsing.

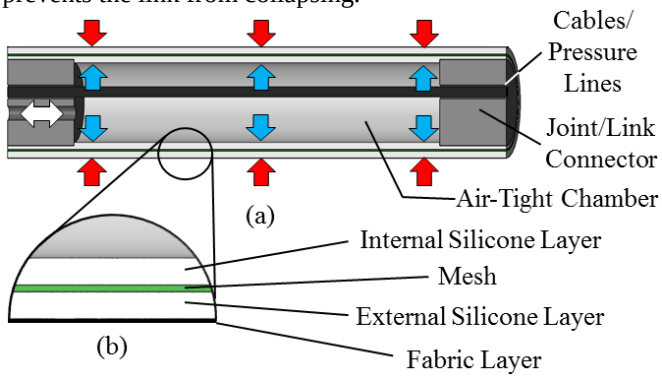

Figure 2 - VSL working principle and design: (a) CAD drawings showing a longitudinal section view of the VSL illustrating the I/O channel for pressurized air (double headed white arrow), the force distribution of the air in pressure inside the internal chamber (azure arrows) and the force distribution of the reaction forces of the link walls (red arrows); (b) subfigure shows a magnified longitudinal section, highlighting the layers composing the wall link.

Links typically present cavities or hollow channels to house cables/tendons allowing routing of these elements along/inside the manipulator body to empower motors and tools on the end effector. The design here proposed maximises the space for cable housing inside the link body providing a large percentage of the link external volume (external diameter of the link 30 mm, internal diameter 25 mm for the presented system, hence almost 70% of the external volume of the link is available).

B. VSL Materials and Fabrication

Based on previous investigations regarding the material choice of the VSL in [26], it was decided to select the following components: Dragon Skin® 20A silicone by Smooth-On Inc. (US) and a Polypropylene (PP) plastic mesh (Figure 3 part I) with diamond shaped texture.

The multiple stages of the fabrication process are shown in Figure 3. Initially, a rectangular sheet of mesh (I) is cut from a larger layer. The longer side is 140 mm in length which will be equivalent to the length of the link. The height is approximately 10 mm longer than the circumference of the cylindrical links being around 80 mm. The additional 10 mm of material is needed in order to provide a 5mm overlap between the two long sides once the mesh is closed in the shape of a cylinder. This overlap allows for soldering the rectangular mesh to a cylindrical shape. The overlapping is kept to minimum in order to minimise the thickness increase, keeping the mesh as isomorph as possible. Hence, by using a commercially available plastic welding tool, a 2 mm solder line was produced on the rolled up rectangular mesh, to form it in the shape of a cylinder (see Figure 3, II).

In the second stage of the fabrication process, the plastic mesh is embedded into a layer of silicone. A two-phase moulding process is applied to cast the silicone on the mesh a cylindrical shape. Figure 4.a shows the components of the first mould used to create the external silicone layer. The cylindrical mesh (II) is slipped over the cylindrical mesh support. The two shells of the mould are then assembled forming a hollow cylinder. Dragon Skin® 20A silicone is mixed, degassed and poured in the outer cylindrical mould. The rolled mesh and its support are inserted into the assembled shells fulfilled with silicone that fills the interstice between the internal and external walls. The entire moulding system is composed of several parts in order to ensure a smooth de-moulding process.

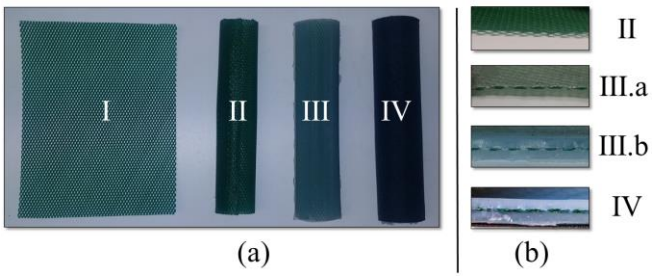

Figure 3 - Fabrication stage of the VSL: subfigure (a) shows how the VSL looks from the outside and subfigure (b) shows how the wall section looks like during the assembly process. I is the mesh before being formed in the shape of a cylinder, II is the mesh soldered and closed in the shape of cylinder, III is the link after the casting of the external silicone layer (III.a) and after casting of the internal layer (III.b) and IV is the finished VSL.

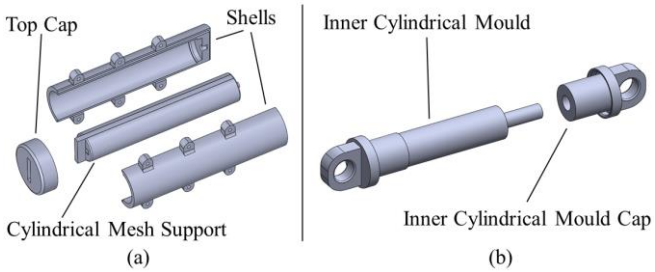

Figure 4 - CAD drawings of the moulds to form the external (a) and the external (b) silicone layers of the lateral walls of the VSL.

Figure 3, III.a shows the resulting mesh in a cylindrical shape and an outer layer of silicone. Now, an internal layer of silicone is added utilizing the mould shown in Figure 4.b. Silicone is poured inside the partially formed link and the inner mould components are inserted from the two sides. This process finally results in the mesh being embedded between two layers of silicone (III.b): the internal layer has a thickness of 1 mm whereas the external thickness is about 1.5 mm. Meanwhile, a rectangular sheet of fine woven nylon fabric is cut and sewn as well in the shape of a cylinder and slipped on the outside of cast link (see Figure 3, IV).

C. Variable Stiffness Anthropomorphic Robot Design

In this paper, we assembled the manipulator shown in Figure 1 . The anthropomorphic robot is composed of two VSL and three rotational joints.

The joints are actuated by: one high torque 360° stepper motor in the base (SY57ST76/0686B, indicated as J1) and by 180° servo motors (HS-7954SH, indicated as J2 and J3). The motors were chosen in order to guarantee a payload on the end effector of 3N in addition to the weight of the two VSLs, the weight of the servo motors and additional 3D printed components. Servomotors were preferred to stepper motors for J2 and J3 due to their smaller weight, given the torque. Furthermore, the torque required on J1 is more than twice the torque required on J3. Hence, a high torque stepper motor was selected for J1 and a lightweight servomotor was selected for J3. All other components of the manipulator have been designed and 3D printed using two different machines: a Stratasys Dimension SST 768 and a ProJet® HD 3000 Plus. The former for components for high resolution components, the latter for the remaining elements.

To guarantee the air-tightness of the VSL chambers, the connections between the joint bases and link extremities have been sealed with silicone glue and reinforced with metal cable ties, as shown in Figure 1. Concerning the hardware of the motor and pressure control, an Arduino Uno board is used. The control scheme is shown in the bottom of Figure 1 . While the servo motors are controlled directly, an additional board is needed to control the stepper motor, hence, an Adafruit motor shield V2, has been added in stack on the Arduino Uno.

Two electro-pneumatic regulators (SMC ITV0030-3BS-Q – Output pressure range 0-5 bar) are used to independently control the pressure level of the two VSLs. A commercially available compressor is used as the regulators' pressure source. Two digital-to-analog converters are used to provide the desired pressure value to the regulators and feedback the pressure reading.

III. EXPERIMENTAL SETUP AND RESULTS ANALYSIS

Two sets of experiments have been designed to evaluate the performance of the VSL and their potential use in industrial settings. In particular, experiments have been conducted to investigate the safety aspect for human-robot interaction.

First the deformation of the VSL is assessed when different loads and pressures are applied. We demonstrate how this soft, stiffness-controllable structure can be approximated fitting the beam model - simplifying the modelling and the control of the VSL and of the overall system.

Second we show how the VSL can be used as a distributed sensor for collision detection. Data retrieved from the pressure sensors of the regulators is analyzed with respect to rapid pressure changes. Hence, collision detection can be integrated without adding any additional hardware to the system.

A. End Effector Workspace Evaluation

To evaluate the stiffness-versus-load effects on the workspace of the VSL manipulator, two series of experiments were conducted: The end effector was loaded using a series of weights (0 N, 0.5 N, 1 N, 1.5 N and 2 N). Each experiment was repeated at five different pressure level (from 0 bar to 2 bar with steps of 0.5 bar). Then, J2 is actuated from 0 to 180° and J3 from 0 to 180°, independently.

In order to evaluate the position of the end effector, an NDI Aurora Electromagnetic Tracking System was used. This system is composed by two elements: a field generator that emits a low intensity electromagnetic field and magnetic trackers to be collocated inside the workspace of the generator. One tracker was mounted on the manipulator's end effector and another one on J2. The results are illustrated in the graphs in Figure 5.

Even though the elongation of the VSLs was measured in the full range of motion of J3 (0° to 180°), the graphs show the positions of the end effector in the 1st quadrant only, given the verified symmetry of the results in the 2nd quadrant. A magnified view is also provided to enhance the readability of the results. In each subfigure of Figure 5, the pressure is fixed (0 bar in Figure 5(a), 1 bar in Figure 5.b and 2 bar in Figure 5.c) (c)) while the load varies, as shown in the labels. The blue circumference in the three graphs is the ideal circumference that has as radius the distance between the magnetic markers placed in the end effector and in J2 and as center J2, when the robot is not loaded and the VSLs are at the pressure used respectively in the three set of experiments. As the graphs show, the overall behavior of the VSL at the different pressure levels is consistent: the higher the load the higher the deformation. Considering an effective length of 140 mm for the VSL (the 183 mm distance shown in the graphs for the reference circumference takes in account the rigid connectors of the VSL mounted on the extremities), a maximum length variation of 5 mm for all the given pressures is detected. Hence, a maximum percentage variation of 3.57 %. This value slightly decreases with the increase of the pressure which is equivalent to the stiffness. Furthermore, the higher the pressure the less noisy the data due the stiffness increase and the consequent more rigid behavior of the VSL.

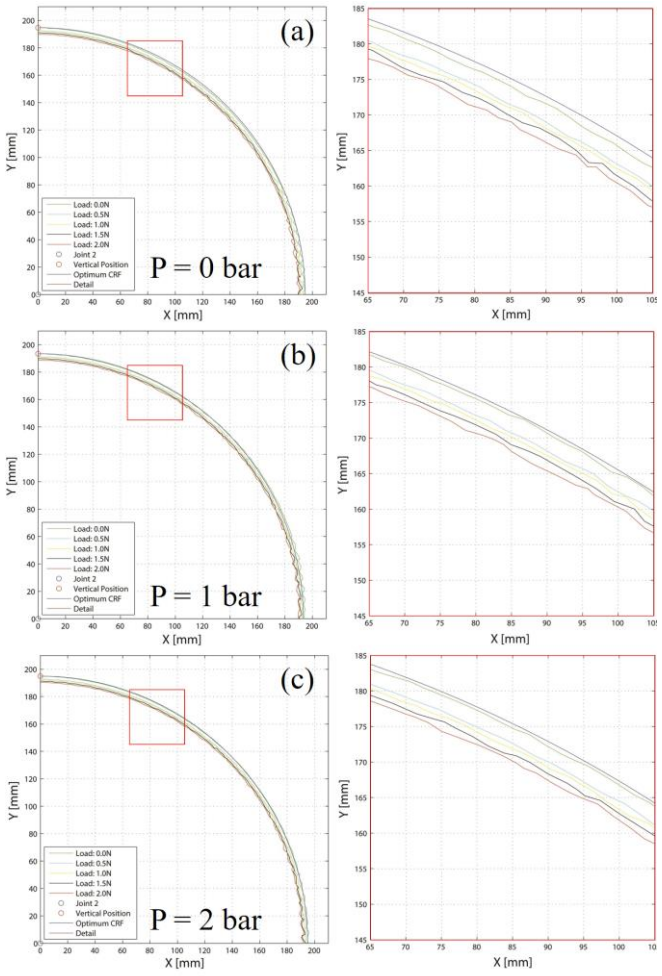

Figure 5 - End effector position in the XY plane (defined as best fit plane for the sequential position of the end effector) when actuating J3 from 0° to 90° (left graphs) when the pressure inside the VSLs are (a) 0 bar, (b) 1 bar and (c) 2 bar. In all graphs, the data is plotted for different load levels on the end effector (0N, 0.5N, 1N, 1.5N and 2N). The reference system is centered in J3. During the experiments, the VSL1 is kept in vertical position; The pressure level of VSL1 and VSL2 is identical. J3 was actuated at a speed of 30°/s. A magnified view of each of the graph on the left is presented in the graphs on the right, showing the content of the red boxes in the main graphs.

It is worth mentioning that thanks to the multi-layer design of the VSL and the structural support of the mesh, a combination of low pressures (0.1 bar) and high loads in horizontal positions do not result in the VSL collapsing.

B. Collision Detection Algorithm

To use the VSLs as distributed sensors to detect collisions, the instant pressure value are measured by the pressure regulator in real time and fed back to the Arduino. The proposed approach is to read the level of pressure inside the VSL and identify a collision by detecting a high change in the pressure values. An algorithm has been implemented (see Algorithm 1). The average pressure is measured over a period T and stored as reference value for the manipulator behaviour when it is not in collision. The idea behind the proposed algorithm is to detect a collision when at least two samples in an experimentally defined time span (y) are above a certain threshold, calculated as a percentage (x) of the average pressure inside the VSL.

Algorithm 1: Pseudocode for Collision Detection

```
for (T=1 ms; T++)
    SumPressure[T] += ReadValueFrom(VSL_2)
    AveragePressure =SumPressure[T]/T
    Threshold = x% (AveragePressure)
    InstantPressure = ReadValueFrom(VSL_2);

    if (InstantPressure >= AveragePressure + Threshold)
        for (y ms)
            Pressure = ReadValueFrom(VSL_2);
            if (Pressure >= Threshold)
                CollisionDetected();
            end if
        end for
end for
```

The experimental setup is shown in Figure 6. Aiming to simulate a collision inside the workspace of the manipulator, the VSL1 was kept in vertical position with J3 moving from 0° to 180°. Approximately at an angle of 145° a rigid object was located. In order to collect force data in the point of collision, an ATI Nano17 Force/Torque sensor was positioned (see Figure 6). The test was conducted both simulating a collision with the point of physical contact being in the middle of the VSL (as in Figure 6) and at the end effector. Both tests were performed with the same angular speed of J3. Both sets of experiments have been repeated ten times in order to evaluate also the success rate of the algorithm. A pressure of 1.4 bar has been selected to be used in these tests. This value can be considered the average pressure level inside the VSL.

The pressure readings were collected from the pressure regulators by Arduino at 2.4 kHz, hence with a sample period of 0.48 ms.

Experimentally, a time span y = 8.4 ms and a percentage threshold x = 1.4 % were defined for the algorithm.

Once the collision occurs, two parallel reactions have been implemented to minimise the interaction force in the point of collision: the link stops and moves away from the subject of the collision. Simultaneously, its pressure is lowered (to 0.5 bar) to significantly reduce its stiffness, providing a softer and safer interaction. In a larger-scale robotic system for industrial settings the combination of these two behaviours can prevent an otherwise harmful/deadly collision between a robot and an operator in its workspace. Table 1 summarises the results obtained from the two set of the experiments proposed in this section, calculating the average values as the average of ten sets of experiments for each of the two tests proposed. Figure 7 illustrates the force and time values listed in the table.

Table 1 - Collision detection data for linear speed at the point of collision, peak force detected and reaction times of the system.

	Link Middle	End Effector
Linear Speed in the Point of Collision [cm/s]	6.65	8.56
Peak Collision Force [N]	5.25	3.43
Detection Time [ms]	110	80
Motion Reaction Time [ms]	120	120
Pressure Reaction Time [ms]	480	480
Total Motion Reaction Time [ms]	230	200
Total Pressure Reaction Time [ms]	590	560

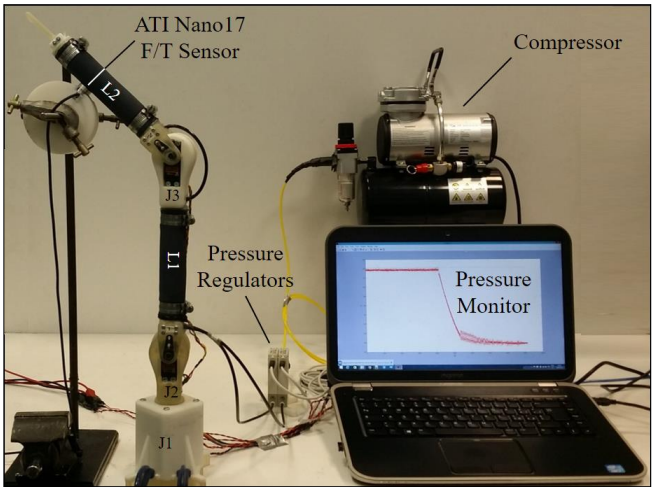

Figure 6 – Overview of the experimental setup for the testing of the collision detection algorithm.

The total motion reaction time and the total pressure reaction time are respectively the sum of the motion reaction time and the pressure reaction time plus the detection time. Based on the results in Table I, it can be concluded that the collision detection algorithm performs more effective at a higher linear speed.

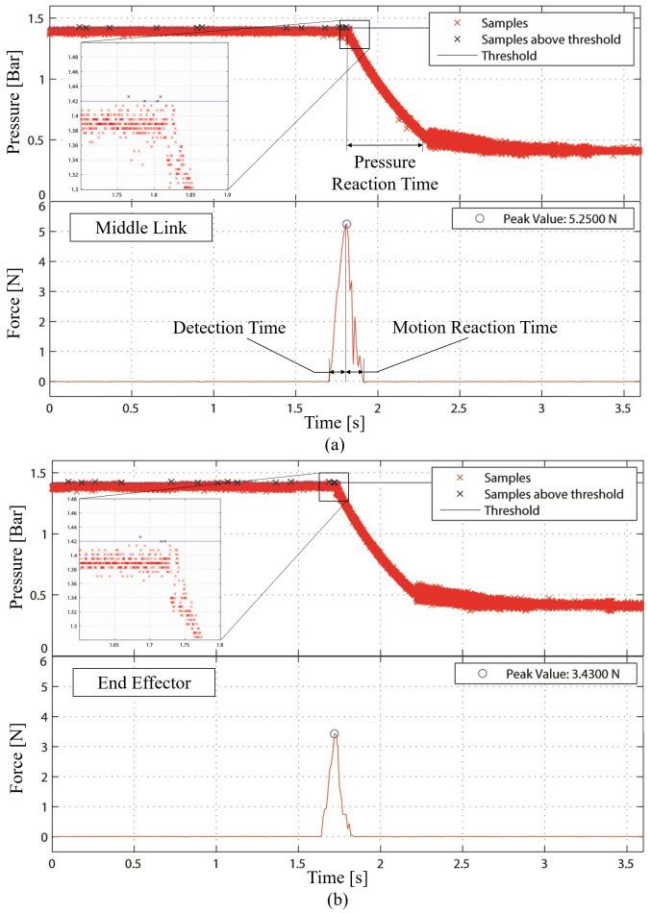

Figure 7 - Collision detection data for different point of impacts: the middle point of VSL2 (a) and the end effector (b). Pressure values collected from the pressure regulator controlling VSL2 and force value collected from the ATI Nano17 force/torque sensor. Force data collected relate to the normal direction as shown in Figure 6.

Not only a decrement of 34.67% on the peak force of impact is measured, but also the time of detection decreases by 27.28 % from the former to the latter case. Due to the higher linear velocity of the impact at the end effector, the variation of pressure recorded in VSL2 shows a more rapid pressure change compared to the middle link case. Hence, a greater amount of samples overcome the threshold consecutively and less time is needed by the system in order to identify the collision, as shown in the magnifications in Figure 7 (a) and (b). With the current system in both cases more than 500ms are needed to depressurize the link to a low stiffness level from the moment of the collision. This time also considers communication limitations of the pressure regulators. Nonetheless, the response time of the overall system as a sensor is just 110ms in the worst case, providing a prompt collision detection considering the performance of the microcontroller used to analyse the data. Furthermore, even though the servomotors used are inexpensive motors for modelling, they allow the system to react to the collision in just over 200ms. The collision detection algorithm performance are demonstrated in the video attached to this submission, where also an overview of the system and a pick and place task are shown.

IV. CONCLUSIONS

In this paper, we proposed a new generation of collaborative robots made of Variable Stiffness Links (VSL). The stiffness of each VSL can be varied over a wide range and, hence, this robotic system offers a novel solution for close, inherently safe collaboration with a human worker.

The links of the described robot are made of a combination of Dragon Skin® 20A silicone and fabric materials. This allows the links to achieve high stiffness values. At the same time, low pressure values result in a compliant robot structure with minimal impact to a human worker in case of collisions. Further, the VSL can also be utilized as distributed sensors that are able to detect collisions. Pressure sensor information of the pressure regulators is monitored. Rapid change in the pressure sensory data will suggest a collision which will then result in immediate stiffness adjustment.

Our future work will focus on advanced filtering of the pressure data to improve collision detection algorithm. The usage of better microcontrollers will be also considered to reduce the detection time. It will be of interest to investigate the interplay of pressure changes when handling payloads and collision detection at the same time. Hence, the aim is to minimize the number of false positives and to simplify the calibration of the controller. Multiple chamber solution will be explored both to allow a more reliable detection of the point of collision and a possibility to control stiffness at specific locations along each link.

REFERENCES

[1] S. Oberer-Treitz, T. Dietz, and A. Verl, "Safety in industrial applications: From fixed fences to direct interaction," in *2013 44th International Symposium on Robotics, ISR 2013*, 2013.

[2] A. J. Baerveldt, "A safety system for close interaction between man and robot," *Saf. Comput. Control Syst. SAFECOMP*, vol. 92, pp. 25–29, 2014.

[3] O. Khatib, "Robots in Human Environments: Basic Autonomous Capabilities," *Int. J. Rob. Res.*, vol. 18, pp. 684–696, 1999.

[4] S. Haddadin, a. Albu-Schaffer, and G. Hirzinger, "Requirements for Safe Robots: Measurements, Analysis and New Insights," *Int. J. Rob. Res.*, vol. 28, no. 11–12, pp. 1507–1527, 2009.

[5] "KUKA Robots website (retrieved on 14.09.2016)." .

[6] "ABB Robotics website (retrieved on 14.09.16)." .

[7] A. De Santis, B. Siciliano, A. De Luca, and A. Bicchi, "An atlas of physical human-robot interaction," *Mechanism and Machine Theory*, vol. 43, no. 3. pp. 253–270, 2008.

[8] H. A. Yanco and J. L. Drury, "A Taxonomy for Human-Robot Interaction," *Engineering*, p. 9, 2002.

[9] "Universal Robots website (retrieved on 14.09.2016)." .

[10] "FerRobotics Compliant Robot Technology website (retrieved on 14.09.2016)." .

[11] "FRANKA EMIKA website (retrieved on 14.09.2016)." .

[12] "Rethink Robotics website (retrieved on 14.09.2016)." .

[13] G. Tonietti, R. Schiavi, and A. Bicchi, "Design and Control of a Variable Stiffness Actuator for Safe and Fast Physical Human/Robot Interaction," *Robotics and Automation, 2005. ICRA 2005. Proceedings of the 2005 IEEE International Conference on*. pp. 526–531, 2005.

[14] R. Ham, T. Sugar, B. Vanderborght, K. Hollander, and D. Lefeber, "Compliant actuator designs," *IEEE Robot. Autom. Mag.*, vol. 16, no. 3, 2009.

[15] A. De Luca and R. Mattone, "Sensorless robot collision detection and hybrid force/motion control," in *Proceedings of the 2005 IEEE international conference on robotics and automation*, 2005, pp. 999–1004.

[16] M. W. Hyun, J. Yoo, S. T. Hwang, J. H. Choi, S. Kang, and S. J. Kim, "Optimal design of a variable stiffness joint using permanent magnets," in *IEEE Transactions on Magnetics*, 2007, vol. 43, no. 6, pp. 2710–2712.

[17] J. Choi, S. Park, W. Lee, and S. C. Kang, "Design of a robot joint with variable stiffness," in *Proceedings - IEEE International Conference on Robotics and Automation*, 2008, pp. 1760–1765.

[18] J. Choi, S. Hong, W. Lee, and S. Kang, "A variable stiffness joint using leaf springs for robot manipulators," in *Proceedings - IEEE International Conference on Robotics and Automation*, 2009, pp. 4363–4368.

[19] D. Silvera-Tawil, D. Rye, and M. Velonaki, "Artificial skin and tactile sensing for socially interactive robots: A review," *Robotics and Autonomous Systems*, vol. 63, no. P3. pp. 230–243, 2015.

[20] R. D. Ponce Wong, J. D. Posner, and V. J. Santos, "Flexible microfluidic normal force sensor skin for tactile feedback," *Sensors Actuators A Phys.*, vol. 179, pp. 62–69, Jun. 2012.

[21] A. Schmitz, P. Maiolino, M. Maggiali, L. Natale, G. Cannata, and G. Metta, "Methods and technologies for the implementation of large-scale robot tactile sensors," *IEEE Trans. Robot.*, vol. 27, no. 3, pp. 389–400, 2011.

[22] D. M. Ebert and D. D. Henrich, "Safe human-robot-cooperation: image-based collision detection for industrial robots," *IEEE/RSJ Int. Conf. Intell. Robot. Syst.*, vol. 2, no. October, pp. 1826–1831, 2002.

[23] S. Sanan, M. H. Ornstein, and C. G. Atkeson, "Physical human interaction for an inflatable manipulator," in *2011 Annual International Conference of the IEEE Engineering in Medicine and Biology Society*, 2011, pp. 7401–7404.

[24] A. Stilli, H. A. Wurdemann, and K. Althoefer, "Shrinkable, stiffness-controllable soft manipulator based on a bio-inspired antagonistic actuation principle," in *IEEE International Conference on Intelligent Robots and Systems*, 2014, pp. 2476–2481.

[25] F. Maghooa, A. Stilli, Y. Noh, K. Althoefer, and H. A. Wurdemann, "Tendon and pressure actuation for a bio-inspired manipulator based on an antagonistic principle," *Robotics and Automation (ICRA), 2015 IEEE International Conference on*. pp. 2556–2561, 2015.

[26] A. Stilli, H. A. Wurdemann, and K. Althoefer, "A Novel Concept for Safe , Stiffness-Controllable Robot Links," *Soft Robot.*, p. soro.2016.0015, 2016.